Published in final edited form as:
Hepatology. 2012 December ; 56(6): 2344–2352. doi:10.1002/hep.25918.

Hepatocyte specific deletion of farnesoid X receptor delays, but does not inhibit liver regeneration after partial hepatectomy in mice

Prachi Borude, **Genea Edwards**, **Chad Walesky**, **Feng Li**, **Xiaochao Ma**, **Bo Kong**, **Grace L. Guo**, and **Udayan Apte**
Department of Pharmacology, Toxicology and Therapeutics, University of Kansas Medical Center, Kansas City, KS

Abstract

Farnesoid X Receptor (FXR), the primary bile acid-sensing nuclear receptor, also plays a role in stimulation of liver regeneration. Whole body deletion of FXR results in significant inhibition of liver regeneration after partial hepatectomy (PHX). FXR is expressed in liver and intestine and recent ChIP-seq analysis indicates that FXR regulates distinct set of genes in a tissue-specific manner. These data raise the question about relative contribution of hepatic and intestinal FXR in regulation of liver regeneration. We studied liver regeneration after PHX in hepatocyte-specific FXR knockout (hepFXR-KO) mice over a time course of 0 to 14 days. Whereas the overall kinetics of liver regrowth in hepFXR-KO mice was unaffected, a delay in peak hepatocyte proliferation from day 2 to day 3 after PHX was observed in the hepFXR-KO mice as compared to Cre^- control mice. Real Time PCR, Western blot and co-IP studies revealed decreased Cyclin D1 expression and decreased association of Cyclin D1 with CDK4 in hepFXR-KO mice after PHX, correlating with decreased phosphorylation of pRb and delayed cell proliferation in the hepFXR-KO livers. The hepFXR-KO mice also exhibited delay in acute hepatic fat accumulation following PHX, which is associated with regulation of cell cycle. Further, a significant delay in HGF-initiated signaling, including AKT, c-myc and ERK-1/2 pathways, was observed in hepFXR-KO mice. UPLC-mass spectroscopy analysis of hepatic bile acids indicated no difference in levels of bile acids in hepFXR-KO and control mice. *In Conclusion,* deletion of hepatic FXR did not completely inhibit but delays liver regeneration after PHX secondary to delayed Cyclin D1 activation.

Keywords

HGF; Fat; Proliferation; Cyclin D1; Bile Acids

Introduction

Liver regeneration is regulated by a complex network of signals involving cytokines, chemokines, growth factors and nuclear receptors (5, 13, 14). Previous studies have demonstrated that Farnesoid X Receptor (FXR), the primary bile acid sensing nuclear receptor, plays a critical role in stimulation of liver regeneration following partial hepatectomy (PHX)(8). FXR is highly expressed in the liver and the intestine, and plays a central role in maintaining bile acid homeostasis (6, 21). Deletion of FXR in the whole body as in FXR knockout (FXR-KO) mice results in massive disruption in bile acid homeostasis

Contact Information: Udayan Apte, PhD, DABT, Department of Pharmacology, Toxicology and Therapeutics, University of Kansas Medical Center, 3901 Rainbow Blvd, MS1018, Kansas City, KS 66160, Tel: (913) 588-9247, uapte@kumc.edu.

leading to higher total bile acids, moderate liver injury, increased oxidative stress and development of spontaneous liver cancers (10, 18, 23). FXR-KO mice also exhibit significant inhibition of liver regeneration following partial hepatectomy highlighting the role of FXR in regulation of liver cell proliferation and tissue repair (8, 12).

Recent studies using ChIP-sequencing have revealed that FXR binds to a distinct set of genes in the liver compared to its binding in the intestine (19). Further, it is known that coordination between hepatic and intestinal FXR signaling is necessary for maintaining bile acid homeostasis in the body and the intestinal FXR-mediated pathway is more critical in suppressing bile acid synthesis than a hepatic FXR-mediated pathway (9). It is clear that FXR signaling in the liver and intestine is distinct and results obtained from whole body modulation of FXR need to be further refined to understand underlying molecular mechanisms.

In the current study, we have determined the contribution of hepatic FXR to liver regeneration following partial hepatectomy using the hepFXR-KO mice. Our data indicate that liver regeneration is regulated by hepatic FXR, but the intestinal FXR likely contributes to regulation of hepatocyte proliferation following partial hepatectomy. We provide evidence that the gut-liver FXR signaling axis plays a critical role in liver regeneration.

Methods

Animals, Surgeries and Tissue Harvesting

The hepFXR-KO mice ($FXR^{loxP/loxP}$; albumin-cre^{+}) and Control ($FXR^{loxP/loxP}$; albumin-cre^{-}) were generated as described before using the cre-lox P system (9). Two to four month old male control and hepFXR-KO mice were used in these studies. All animals were housed in Association for Assessment and Accreditation of Laboratory Animal Care-accredited facilities at the University of Kansas Medical Center under a standard 12-hr light/dark cycle with access to chow and water *ad libitum*. The Institutional Animal Care and Use Committee at University of Kansas Medical Center approved all studies.

Partial hepatectomy surgeries were performed as previously described (1). All surgeries were performed between 9:00 am and 11:00 am in the morning. Mice were killed at 0, 1, 2, 3, 5, 7, and 14 days post-PHX by cervical dislocation under isofluorane anesthesia and livers were collected. The liver weights and body weights at the time of animal sacrifice were used to calculate the liver-to-body-weight ratios. The results obtained were the mean of three to five different animals per time point.

Part of liver tissue was fixed in 10% neutral buffered formalin for 48 h, further processed to obtain paraffin blocks and 4μm thick sections. A piece of liver was frozen in OCT and used to obtain fresh frozen sections. Approximately 100 mg liver tissue was used to prepare fresh nuclear and cytoplasmic protein extracts using the NE-PER Nuclear and Cytoplasmic Extraction Kit (Pierce, Rockford, IL). The remaining liver tissue was frozen in liquid N_2, and stored at −80°C until used to prepare RIPA protein extracts.

Antibodies

All primary and secondary antibodies used for Western blot analysis were obtained from Cell Signaling Technologies (Danvers, MA) and biotinylated secondary antibodies for immunohistochemistry were purchased from Jackson Immunoresearch (West Grove, PA). The antibodies used and their catalogue numbers are provided in table 1.

Protein Isolation and Western Blotting

Western blot analysis was performed as previously published without any modifications (22). Briefly, RIPA protein extracts were prepared from frozen liver tissues and protein concentration was estimated by BCA method (Thermo Fisher). Fifty micrograms of total protein per well was used for Western blot analysis.

PCNA Immunohistochemistry and Oil Red O Staining

Paraffin-embedded liver sections (4 μm thick) were used for immunohistochemical detection of PCNA as described before (22). For Oil Red O staining, 5 μm thick frozen sections were used and staining was performed as previously described (11).

Real Time PCR

Total RNA was isolated from control and hepFXR-KO livers using Trizol method according to the manufacturer's protocol (Sigma, St. Louis, MO) and converted to cDNA as previously described (22). mRNA levels of various genes was determined using TaqMan-based Real Time PCR analysis using commercially available TaqMan Gene Expression Assays (Life Technologies previously known as Applied Biosystems, Carlsbad, CA) on the Applied Biosystems Prism 7300 Real-time PCR Instrument as described previously (22). Rplp0 gene expression in the same samples was used for data normalization.

Bile Acid Analysis

Bile acids were analyzed by UPLC-MS (Waters, Milford, MA) as described before (25). Briefly, individual bile acid was separated by a 100 mm × 2.1 mm (Acquity 1.7 μm) UPLC BEH C-18 column. The flow rate of the mobile phase was 0.3 mL/min with a gradient ranging from 2% to 98% aqueous acetonitrile containing 0.1% formic acid in a 10-min run. MS was operated in a negative mode with electrospray ionization. The source temperature and desolvation temperature were set at 120 °C and 350 °C, respectively. The capillary voltage and the cone voltage were set at 3.0 kV and 28 V. Nitrogen was applied as the cone gas (10 liters/hour) and desolvation gas (700 liters/hour). Argon was applied as the collision gas.

Statistical Analysis

Data presented in the form of bar graphs show mean ± SD. To determine statistically significant difference between groups, paired Student's T-test was used. Difference between groups was considered statistically significant at $P<0.05$. The different degrees of significance was indicated as follows in the bar graphs- *$P<0.05$; **$P<0.01$; ***$P<0.001$

Results

Delayed peak proliferation in hepFXR-KO mice

The liver weight to body weight ratio analysis in control and hepFXR-KO mice indicated no overall difference in the rate of liver regrowth following PHX over the time course of 0 to 14 days (Fig. 1A). To determine the change in hepatic cell proliferation following PHX we stained liver sections from control and hepFXR-KO mice for PCNA and determined the percentage of cells in cell cycle (Fig. 1B and 2). PCNA analysis revealed a delay in peak of cell proliferation in hepFXR-KO mice. In control mice, peak cell proliferation was observed at day 2 after PHX, which was delayed to day 2 after PHX in the hepFXR-KO mice. Cell proliferation declined significantly in both genotypes at day 7 after PHX but a moderate increase in cell proliferation was observed in the hepFXR-KO mice at day 14 after PHX.

Decreased Cyclin D1 expression in hepFXR-KO after PHX

To determine the mechanism underlying delayed cell proliferation in hepFXR-KO mice, we determined levels of core cell cycle proteins including Cyclin D1, CDK4 and phospho-Rb. A marked increase in Cyclin D1 protein was observed at day 1 after PHX in control mice, which remained increased until day 7 after PHX. A similar increase in Cyclin D1 protein expression was observed in hepFXR-KO mice at day 2 after PHX. However, a marked reduction of Cyclin D1 protein expression in the liver of hepFXR-KO mice was shown at day 2 as compared to control mice (Fig. 3B). The decrease in Cyclin D1 protein was accompanied by decreased Cyclin D1 gene expression at day 2 after PHX in hepFXR-KO mice (Fig. 3A). Both mRNA and protein expression of Cyclin D1 increased at day 3 after PHX and was similar to that observed in control mice. Western blot analysis revealed that levels of CDK4, the catalytic partner of Cyclin D1, were moderately decreased at days 2 and 3 after PHX in hepFXR-KO mice as compared to control (Fig. 3B). These changes were correlated with complete lack of phosphorylated Rb (phospho-Rb) protein, necessary for initiation of cell cycle progression, in the hepFXR-KO mice at days 1 and 2 after PHX (Fig. 3B). We observed increased phospho-Rb levels at day 3 after PHX in hepFXR-KO mice, coinciding with increased cell proliferation at that time point.

Interestingly, at day 1 after PHX in hepFXR-KO mice, we observed the presence of significant Cyclin D1 protein and CDK4, which form the active complex required for phosphorylation of Rb. However, we could not detect any phospho-Rb protein at day 1 after PHX in hepFXR-KO mice by Western blot. To decipher these data we performed co-IP studies on Cylcin D1 and CDK4 in control and hepFXR-KO mouse livers at day 2 after PHX (Fig. 3C and D). The data indicate a decreased association of Cyclin D1 with CDK4 in hepFXR-KO mice as compared to the control mice at day 1 after PHX. These data indicate that lack of phospho-Rb and cell proliferation at day 1 after PHX, despite the presence of Cyclin D1 and CDK4, is due to decreased association of these two components of the phosphorylation machinery.

Cell cycle inhibitors such as p21 and p27 are known to inhibit Cyclin D1-CDK4 complex activity resulting in decreased phosphorylation of Rb. Therefore; we determined levels of p21 and p27 protein in control and hepFXR-KO mice over a time course after PHX. Whereas the data revealed difference in the pattern of p21 and p27 expression following PHX between control and hepFXR-KO mice, no correlation was found in the delayed cell proliferation in hepFXR-KO mice livers and the expression of p21 or p27.

Delayed activation of HGF-mediated Signaling in hepFXR-KO mice after PHX

HGF is one of the primary mitogens critical for proper liver regeneration. HGF binds to its receptor c-Met and initiates a cascade of pro-mitogenic signaling. We determined the changes in HGF signaling axis in Control and hepFXR-KO mice livers following PHX. A marked increase in HGF mRNA was seen at day 2 after PHX in the control mice consistent with previous reports. In contrast, HGF mRNA peaked at day 3 after PHX in the hepFXR-KO mice (Fig 4A). Furthermore, a significantly higher protein expression of c-Met was observed at days 3 and 5 after PHX in the hepFXR-KO livers as compared to control mice (Fig. 4B). Moreover, we determined the activation of three major downstream MAPK mediators, namely ERK-1/2, AKT and p38 kinases, and the data indicated a marked increase in activated (phosphorylated) forms of AKT and ERK-1/2 kinases in hepFXR-KO mice at day 3 after PHX. We did not observe any difference in p38 kinase expression and activation between control and hepFXR-KO mice at any time point (Fig 4C). Interestingly, an increase in both total and phosphorylated forms of AKT protein was observed after PHX, which was significantly higher in hepFXR-KO mice (Fig. 4E). The ratio of phosphorylated to total AKT indicated a significant activation at day 1 after PHX in control mice, which was

delayed till day 3 after PHX in the hepFXR-KO mice (Fig. 4F). Finally, we observed delayed increase in two well known pro-mitogenic genes including c-Myc (Fig. 4B) and c-Jun (Fig. 4D) at day 3 after PHX in the hepFXR-KO mice.

Delayed acute fat accumulation following PHX in hepFXR-KO mice

Previous studies have demonstrated that acute fat accumulation in hepatocytes of the regenerating livers is critical for proper hepatocyte proliferation during liver regeneration (7, 17). Because we observed changes in fat droplet accumulation in the hepFXR-KO mice, we further determined to what degree FXR deficiency affects acute fat accumulation. The results indicate an extensive lipid droplet accumulation in control mouse livers at day 1 after PHX, which disappeared at later time points. Fat accumulation was mostly absent in the hepFXR-KO mouse livers at day 1 after PHX, but increased moderately at day 2 after PHX. The hepFXR-KO mouse livers have extensive fat accumulation at day 3 after PHX, which is delayed for day 2 compared to the control mice (Fig. 5A). To further investigate this delay in acute fat accumulation in hepFXR-KO mice, we determined the mRNA expression of a number of genes involved in fat mobilization and metabolism. Significant changes were shown in two genes associated with increased fat accumulation following PHX, CFD and aP2 (Fig 5B and C). The data indicate that CFD, a gene associated with fat uptake in the liver following PHX, increased significantly in control mice at day 1 after PHX, but not in hepFXR-KO mice at any of the time points studied. Further, mRNA levels of aP2, a gene associated with adipocyte fat mobilization, were increased significantly in the hepFXR-KO mice at days 2 and 3 after PHX coinciding with increase in fat accumulation.

No significant difference in bile acid levels in control and hepFXR-KO mice after PH

One of the main physiological changes observed in whole body FXR-KO mice is the 4-fold increase in total bile acid concentration, which remain elevated in the FXR-KO mice after PHX. To study whether the delay in liver regeneration in hepFXR-KO mice is related to change in bile acid concentration or isoforms, we determined hepatic concentrations of major hepatic bile acids, including α-MCA, β-MCA, ε-MCA, T- β-MCA and TCA. However, no significant difference was observed in these bile acid levels between control and hepFXR-KO mice (Fig. 6).

Discussion

FXR is a nuclear receptor involved in a variety of pathophysiological processes, including bile acid homeostasis, pathogenesis of diseases (insulin resistance, metabolic syndrome and hepatocellular carcinoma), and liver regeneration (4, 6, 20, 21, 24). Previous studies have demonstrated that FXR plays a critical role in liver regeneration after partial hepatectomy as well as after chemical induced injury (8, 12). FXR is expressed both in the gut and in the liver, and it is known that coordinated gut-liver signaling by FXR is crucial for many of its effects, including regulation of bile acid synthesis (9). Recent studies have demonstrated that hepatic FXR and gut FXR regulate a distinct set of target genes. Further, development of organ specific knockout mice has allowed investigators to determine the relative contribution of hepatic vs. gut FXR in the regulation of pathophysiological processes (19). In the present study, we determined the role of hepatic FXR in regulating liver regeneration after PHX. Our data indicate that hepatic FXR plays a limited role in regulation of liver regeneration and the regenerative defects observed in whole of FXR-KO mice are likely due to disruption of gut-liver FXR signaling.

Our studies demonstrated a 24-hr delay in peak proliferation following PHX in the hepFXR-KO mice. This delay was secondary to decreased Cyclin D1 expression in the hepFXR-KO mice. Interestingly, ChIP-seq analysis of FXR in the liver indicates that FXR has a potential

binding site on Cyclin D1 promoter, which was confirmed by ChIP analysis (data not shown). However, we did not observe decrease in Cyclin D1 expression at 1 day after PHX, but observed significant decline in Cyclin D1 expression only at day 2 after PHX in hepFXR-KO mice. These data suggest that FXR may not regulate initial activation of Cyclin D1 but may be involved in sustained Cyclin D1 activation following PHX.

HGF is a primary mitogen for hepatocytes and plays a critical role in hepatocyte proliferation during regeneration (3, 13). HGF binds to its receptor c-Met, which activates a plethora of downstream pro-mitogenic kinase signaling (15). Our data indicate a significant delay in HGF expression and downstream signaling consistent with delayed cell proliferation in the hepFXR-KO mice. However, the exact role of FXR in regulating HGF signaling currently remains unknown. Previous ChIP-seq studies on FXR target genes in the liver indicate that c-Met is a potential target of FXR in the liver (19). Other studies have shown that HGF can stimulate its own gene expression via binding to c-Met and downstream activation of AP1 transcription factor (a complex of c-Fos and c-Jun) (2, 16). Our data indicate a delayed increase in both c-Met and c-Jun (a part of AP1) in the hepFXR-KO mice after PHX coinciding with increased HGF gene expression. It is plausible that the delay in HGF expression observed in the hepFXR-KO mice may be secondary to delayed activation of c-Met-AP1 signaling axis resulting in delayed transcriptional upregulation of HGF. Additionally, HGF expression can be stimulated by cytokines such as IL-6, which is also a putative target of FXR (19).

A serendipitous observation in our studies was the delayed fat accumulation in the hepFXR-KO mice after PHX. Previous work has demonstrated the acute fat accumulation within first 24 hr after PHX is essential for timely cell proliferation and liver regeneration (7, 17). This acute fat accumulation is shown to be associated with genes such as aP-2, CFD and others. Our results indicate that delay in fat accumulation in hepFXR-KO mice coincides with delayed cell proliferation and is consistent with delayed induction of aP-2 and CFD, the genes involved in fat accumulation after PHX. These data suggest that FXR plays a crucial role in hepatic fat accumulation after PHX and supports the energy requirement for the ongoing cell proliferation. However, ChIP-seq analysis did not show any of these genes as potential targets of FXR indicating an indirect role of FXR in hepatic fat accumulation.

Further, we investigated to what degree, delayed regeneration in the hepFXR-KO mice is due to changes in bile acids in these mice. Previous studies have shown that whole body FXR-KO mice have 4-fold higher total bile acids, which further increase after PHX (8, 18). Interestingly, the hepFXR-KO mice do not have the increase in bile acids observed in the whole body FXR-KO mice (9). Our data indicate no difference in changes in hepatic bile acids in control vs. hepFXR-KO mice, ruling out the involvement of bile acids in the observed delay in regeneration.

In conclusion, our study indicates that FXR plays a multi-faceted role in regulation of hepatocyte proliferation including stimulating Cyclin D1, modulating HGF signaling and mobilization of acute hepatic fat accumulation necessary for proper liver regeneration. These data indicate that regulation of liver regeneration after PHX by FXR is likely dependent on the gut-liver FXR signaling axis and not on the hepatic FXR alone. These studies highlight the complex multi-pathway signaling involved in regulation of liver regeneration after PHX and suggest a strong role for metabolic signals in initiation and termination of liver regeneration.

Acknowledgments

Financial Support: These studies were supported by NIH - P20 RR021940 (Udayan Apte and Grace L. Guo), AASLD/ALF Liver Scholar Award (Udayan Apte), R01 DK031343 and KU endowment (Grace Guo).

List of Abbreviations

FXR	Farnesoid X Receptor
hepFXR-KO	hepatocyte specific FXR knockout mice
HGF	hepatocyte growth factor

References

1. Apte U, Gkretsi V, Bowen WC, Mars WM, Luo JH, Donthamsetty S, Orr A, Monga SP, Wu C, Michalopoulos GK. Enhanced liver regeneration following changes induced by hepatocyte-specific genetic ablation of integrin-linked kinase. Hepatology. 2009; 50:844–851. [PubMed: 19575460]
2. Bell AW, Jiang JG, Chen Q, Liu Y, Zarnegar R. The upstream regulatory regions of the hepatocyte growth factor gene promoter are essential for itsexpression in transgenic mice. J Biol Chem. 1998; 273:6900–6908. [PubMed: 9506994]
3. Block GD, Locker J, Bowen WC, Petersen BE, Katyal S, Strom SC, Riley T, Howard TA, Michalopoulos GK. Population expansion, clonal growth, and specific differentiation patterns in primary cultures of hepatocytes induced by HGF/SF, EGF and TGF alpha in a chemically defined (HGM) medium. J Cell Biol. 1996; 132:1133–1149. [PubMed: 8601590]
4. Eloranta JJ, Kullak-Ublick GA. The role of FXR in disorders of bile acid homeostasis. Physiology (Bethesda). 2008; 23:286–295. [PubMed: 18927204]
5. Fausto N, Campbell JS, Riehle KJ. Liver regeneration. Hepatology. 2006; 43:S45–53. [PubMed: 16447274]
6. Gadaleta RM, van Mil SW, Oldenburg B, Siersema PD, Klomp LW, van Erpecum KJ. Bile acids and their nuclear receptor FXR: Relevance for hepatobiliary and gastrointestinal disease. Biochim Biophys Acta. 2010; 1801:683–692. [PubMed: 20399894]
7. Gazit V, Weymann A, Hartman E, Finck BN, Hruz PW, Tzekov A, Rudnick DA. Liver regeneration is impaired in lipodystrophic fatty liver dystrophy mice. Hepatology. 2010; 52:2109–2117. [PubMed: 20967828]
8. Huang W, Ma K, Zhang J, Qatanani M, Cuvillier J, Liu J, Dong B, Huang X, Moore DD. Nuclear receptor-dependent bile acid signaling is required for normal liver regeneration. Science. 2006; 312:233–236. [PubMed: 16614213]
9. Kim I, Ahn SH, Inagaki T, Choi M, Ito S, Guo GL, Kliewer SA, Gonzalez FJ. Differential regulation of bile acid homeostasis by the farnesoid X receptor in liver and intestine. J Lipid Res. 2007; 48:2664–2672. [PubMed: 17720959]
10. Kim I, Morimura K, Shah Y, Yang Q, Ward JM, Gonzalez FJ. Spontaneous hepatocarcinogenesis in farnesoid X receptor-null mice. Carcinogenesis. 2007; 28:940–946. [PubMed: 17183066]
11. Kong B, Luyendyk JP, Tawfik O, Guo GL. Farnesoid X receptor deficiency induces nonalcoholic steatohepatitis in low-density lipoprotein receptor-knockout mice fed ahigh-fat diet. J Pharmacol Exp Ther. 2009; 328:116–122. [PubMed: 18948497]
12. Meng Z, Wang Y, Wang L, Jin W, Liu N, Pan H, Liu L, Wagman L, Forman BM, Huang W. FXR regulates liver repair after CCl4-induced toxic injury. Mol Endocrinol. 2010; 24:886–897. [PubMed: 20211986]
13. Michalopoulos GK. Liver regeneration. J Cell Physiol. 2007; 213:286–300. [PubMed: 17559071]
14. Michalopoulos GK, DeFrances MC. Liver regeneration. Science. 1997; 276:60–66. [PubMed: 9082986]
15. Nakamura T, Sakai K, Nakamura T, Matsumoto K. Hepatocyte growth factor twenty years on: Much more than a growth factor. J Gastroenterol Hepatol. 2011; 26 (Suppl 1):188–202. [PubMed: 21199531]
16. Seol DW, Chen Q, Zarnegar R. Transcriptional activation of the hepatocyte growth factor receptor (c-met) gene by its ligand (hepatocyte growth factor) is mediated through AP-1. Oncogene. 2000; 19:1132–1137. [PubMed: 10713700]

17. Shteyer E, Liao Y, Muglia LJ, Hruz PW, Rudnick DA. Disruption of hepatic adipogenesis is associated with impaired liver regeneration in mice. Hepatology. 2004; 40:1322–1332. [PubMed: 15565660]
18. Sinal CJ, Tohkin M, Miyata M, Ward JM, Lambert G, Gonzalez FJ. Targeted disruption of the nuclear receptor FXR/BAR impairs bile acid and lipid homeostasis. Cell. 2000; 102:731–744. [PubMed: 11030617]
19. Thomas AM, Hart SN, Kong B, Fang J, Zhong XB, Guo GL. Genome-wide tissue-specific farnesoid X receptor binding in mouse liver and intestine. Hepatology. 2010; 51:1410–1419. [PubMed: 20091679]
20. Trauner M, Claudel T, Fickert P, Moustafa T, Wagner M. Bile acids as regulators of hepatic lipid and glucose metabolism. Dig Dis. 2010; 28:220–224. [PubMed: 20460915]
21. Wang YD, Chen WD, Moore DD, Huang W. FXR: a metabolic regulator and cell protector. Cell Res. 2008; 18:1087–1095. [PubMed: 18825165]
22. Wolfe A, Thomas A, Edwards G, Jaseja R, Guo GL, Apte U. Increased Activation of Wnt/{beta}-catenin Pathway in Spontaneous Hepatocellular Carcinoma observed in Farnesoid X Receptor Knockout Mice. J Pharmacol Exp Ther. 2011 (In Press).
23. Yang F, Huang X, Yi T, Yen Y, Moore DD, Huang W. Spontaneous development of liver tumors in the absence of the bile acid receptor farnesoid X receptor. Cancer Res. 2007; 67:863–867. [PubMed: 17283114]
24. Zhang Y, Edwards PA. FXR signaling in metabolic disease. FEBS Lett. 2008; 582:10–18. [PubMed: 18023284]
25. Zhang Y, Klaassen CD. Effects of feeding bile acids and a bile acid sequestrant on hepatic bile acid composition in mice. J Lipid Res. 2010; 51:3230–3242. [PubMed: 20671298]

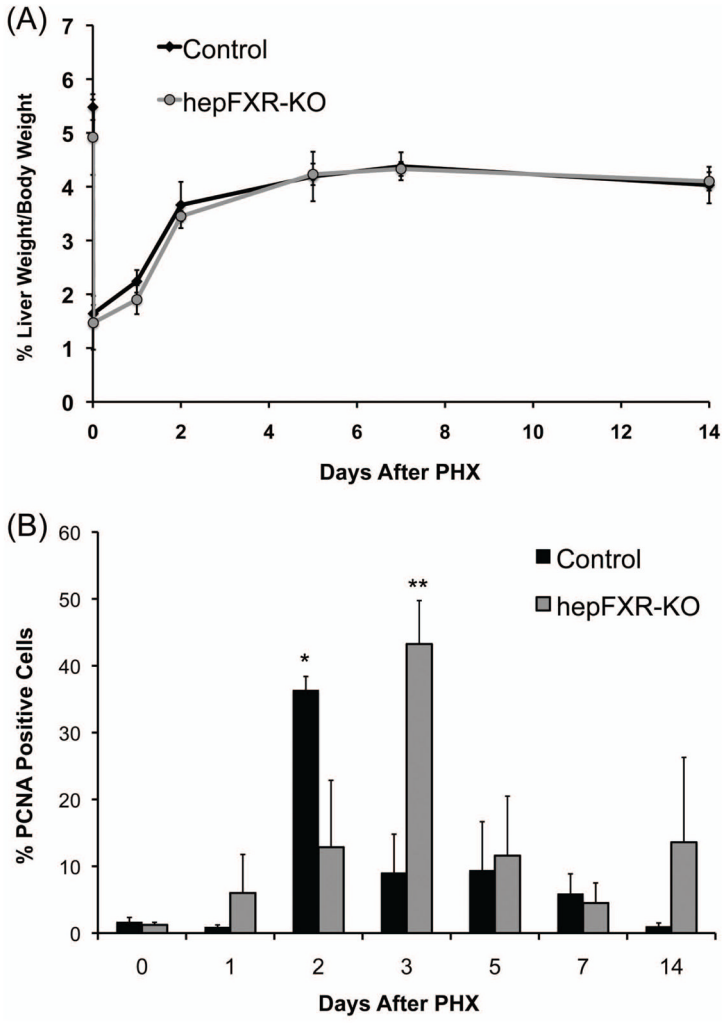

Figure 1.

Liver regeneration after partial hepatectomy is not inhibited but delayed in hepFXR-KO mice. (A) Liver weight to body weight ratio analysis in control and hepFXR-KO mice over a time course of 0 to 14 days after PHX. (B) Percentage of PCNA-positive cells in the livers of Control and hepFXR-KO mice over a time course after PHX. The different degrees of significance was indicated as follows in the graphs- *P<0.05; **P<0.01; ***P<0.001

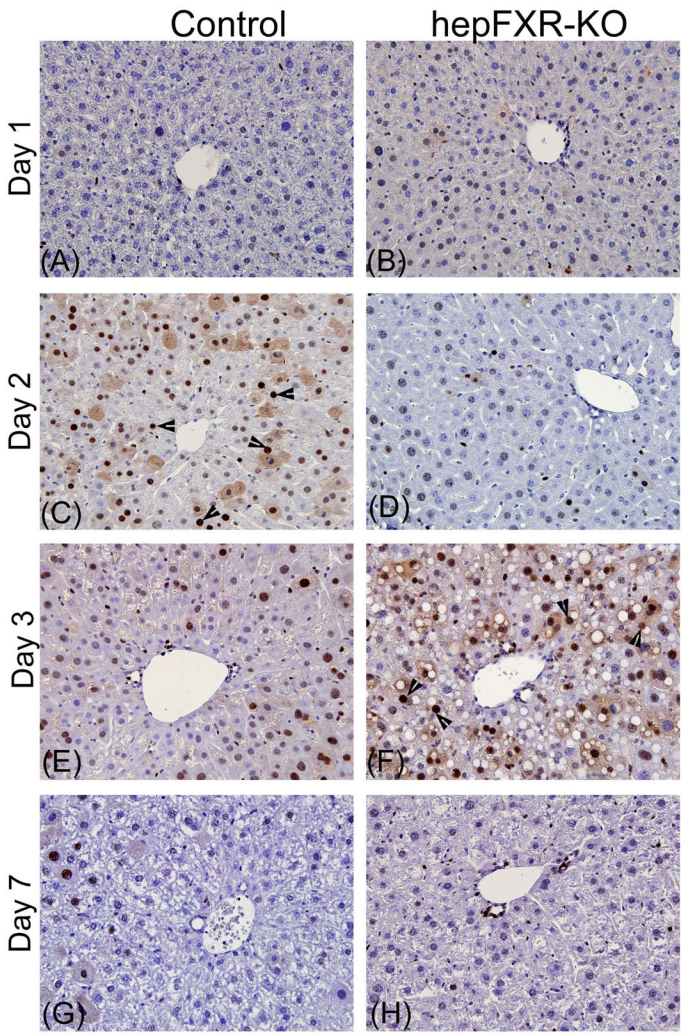

Figure 2.
Delayed peak proliferation in the hepFXR-KO mice after PHX. Representative photomicrographs of PCNA immunohistochemical staining of liver sections from Control (A, C, E, and G) and hepFXR-KO (B, D, F, and H) mice at 1, 2, 3 and 7 days after PHX. Arrowheads point to cells in S-phase.

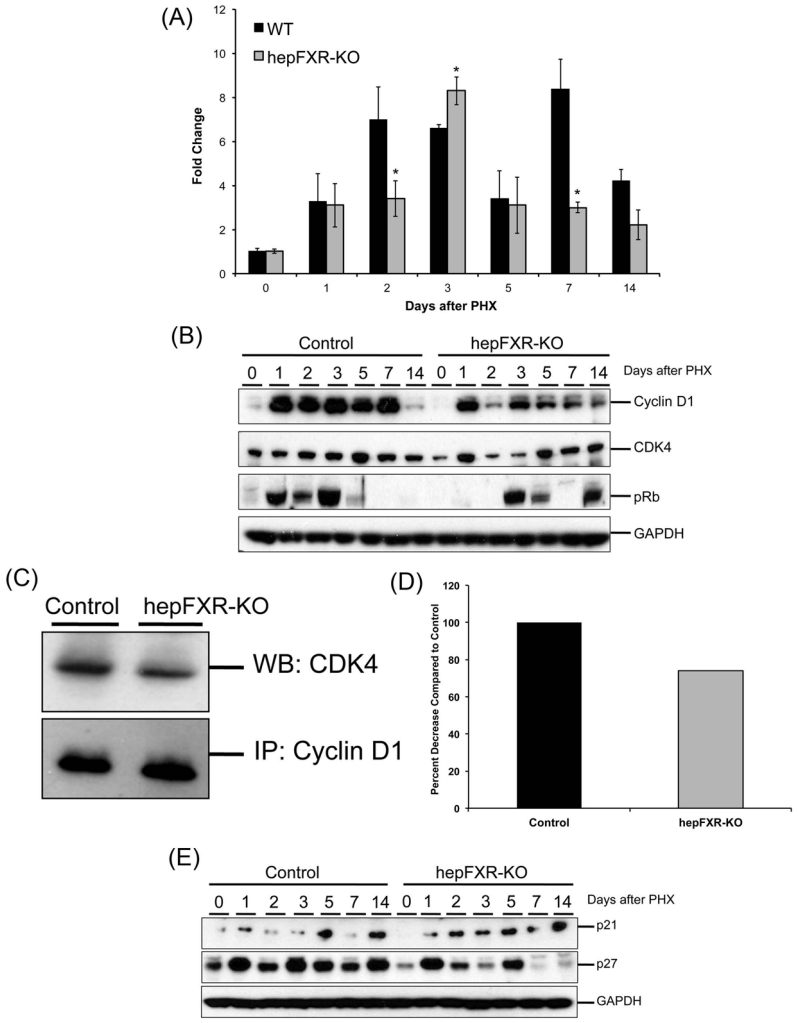

Figure 3.

Delayed Cyclin D1 expression and phosphorylation of Rb in hepFXR-KO mice after PHX. (A) Real Time PCR analysis of Cyclin D1 mRNA in the liver of Control and hepFXR-KO mice after PHX. *P<0.5 (B) Western blot analysis of Cyclin D1, CDK4 and pRb using RIPA extract of Control and hepFXR-KO livers obtained at various time points after PHX. (C) Co-IP analysis of CDK4-Cyclin D1 complex formation at 1 day after PHX in Control and hepFXR-KO mice. (D) Densitometric analysis of the co-IP blots (E) Western blot analysis of cell cycle inhibitors p21 and p27 using RIPA extract of Control and hepFXR-KO livers obtained at various time points after PHX.

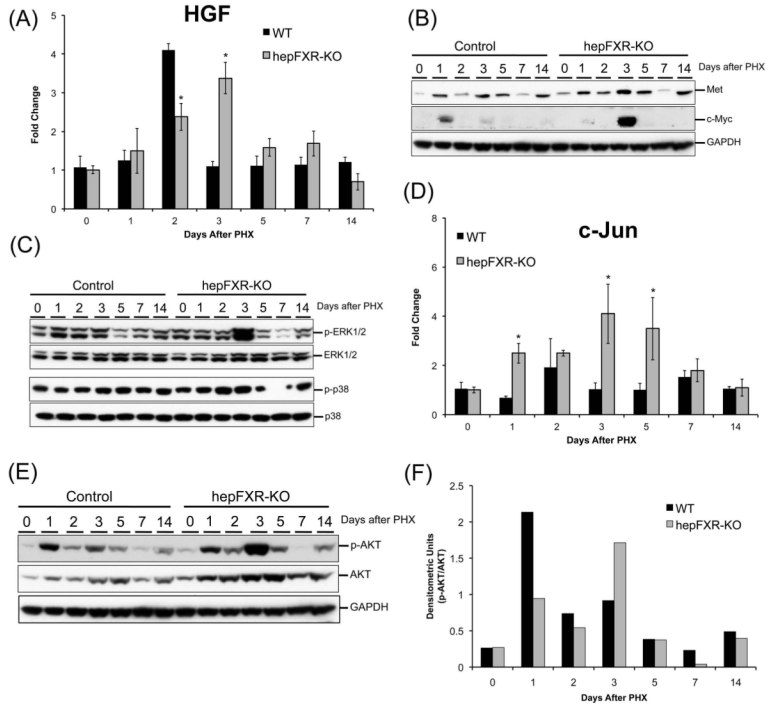

Figure 4.

Delayed signaling via HGF signaling axis in hepFXR-KO mice after PHX. (A) Real Time PCR analysis of HGF in Control and hepFXR-KO livers after PHX. The different degrees of significance was indicated as follows in the graphs- *P<0.05; **P<0.01; ***P<0.001. Western blot analysis of Met and c-Myc (B), ERK-1/2, phosphorylated ERK1/2, p38 and phosphorylated p38 (C) using RIPA extract of Control and hepFXR-KO livers obtained at various time points after PHX. (D) Real time PCR analysis of c-Jun mRNA in Control and hepFXR-KO mice after PHX. The different degrees of significance was indicated as follows in the graphs- *P<0.05; **P<0.01; ***P<0.001. (E) Western blot analysis of total and phosphorylated AKT using RIPA extract of Control and hepFXR-KO livers obtained at various time points after PHX. The ratio of total and phospho-AKT is shown in the bar graph in (F).

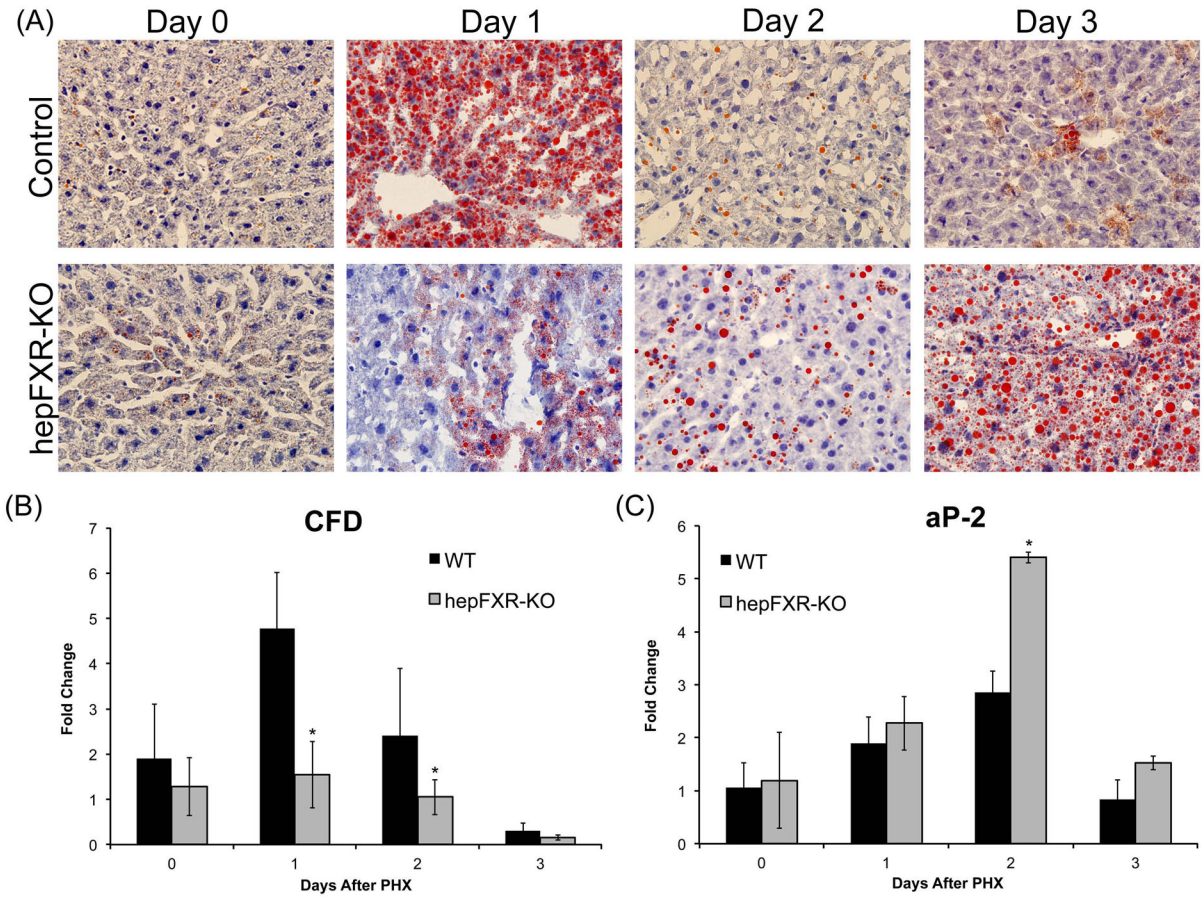

Figure 5.

Delayed fat accumulation in hepFXR-KO mice after PHX. (A) Representative photomicrographs of fresh frozen liver sections stained for Oil Red O from Control and hepFXR-KO mice at 1, 2 and 3 days after PHX. Real Time PCR analysis of CFD (B) and aP2 (C) mRNA in Control and hepFXR-KO mice after PHX. The different degrees of significance was indicated as follows in the graphs- *P<0.05; **P<0.01; ***P<0.001.

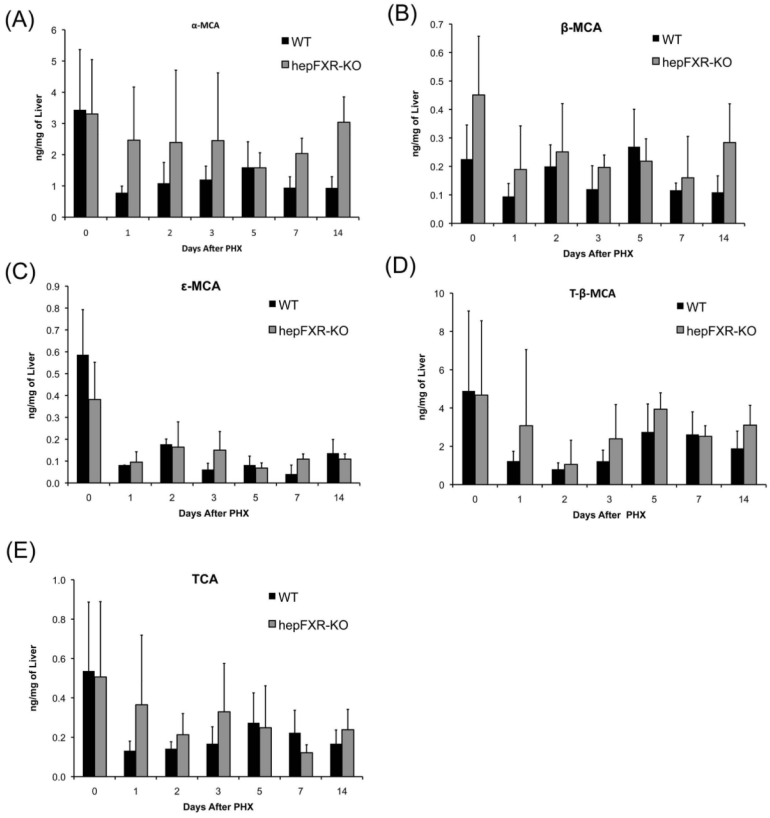

Figure 6.

No difference in hepatic bile acid content between Control and hepFXR-KO mice. Hepatic levels of α-MCA (A), β-MCA (B), ε-MCA (C), T-β-MCA (D), and TCA (E) in the livers of Control and hepFXR-KO mice over a time course of 0 to 14 days after PHX.

Table 1

Antibodies used in this study and their catalog numbers

Name	Cell Signaling Technologies Catalog #
Cyclin D1	2978
CDK4	2906
pRb	9308
p21	2947
p27	3688
c-Met	4560
c-Myc	5606
ERK1/2	9102
Phospho-ERK1/2	4376
p38	9212
Phospho-p38	9211
AKT	4691
Phospho-AKT	9271
GAPDH	2118